Tikrit Journal of Engineering Sciences (2025); 32(2): 1767
DOI: http://doi.org/10.25130/tjes.32.2.8

IRAQI Academic Scientific Journals

ISSN: 1813-162X (Print); 2312-7589 (Online)

Tikrit Journal of Engineering Sciences

available online at: http://www.tj-es.com

TJES Tikrit Journal of Engineering Sciences

Performance Evaluation and Modeling of L1 GPS Receiver and Signal Tracking

Abdullah Khalid Ahmed *, Mohammed AlMahamdy, Naser Al-Falahy

Department of Electrical Engineering, Engineering College, University of Anbar, Anbar, Iraq.

Keywords:

Carrier tracking; Code tracking; Gold code; GPS signal; Pseudo ranging.

Highlights:

- *Gold codes are a better solution for preventing interference since they have less cross-correlation than PN codes.*
- *Even in situations where carrier tracking fails to track the arriving signal, receivers can still decode messages because of the narrow bandwidth of the code tracking loop.*
- *The bounded cross-correlation of the Gold code results significantly improves receiver performance.*
- *The received navigation data has a higher and more stable magnitude in dBW/Hz, making it easy to recover.*

ARTICLE INFO

Article history:

Received	06 Oct.	2023
Received in revised form	28 Jan.	2024
Accepted	17 Apr.	2024
Final Proofreading	19 Oct.	2024
Available online	17 May	2025

Citation: Ahmed AK, AlMahamdy M, Al-Falahy N. **Performance Evaluation and Modeling of L1 GPS Receiver and Signal Tracking**. *Tikrit Journal of Engineering Sciences* 2025; **32**(2): 1767. http://doi.org/10.25130/tjes.32.2.8

***Corresponding author:**

Abdullah Khalid Ahmed

Department of Electrical Engineering, Engineering College, University of Anbar, Anbar, Iraq.

Abstract: Direct Sequence Spread Spectrum (DSSS) has high immunity against noise due to the great spreading gain of the pseudo-noise (PN) code. The Global Positioning System (GPS) satellites send navigation messages at the L1 frequency band, where coarse acquisition codes are embedded within these messages. Two scenarios are evaluated for navigation data tracking: phase tracking and code tracking processes. The coded data is recovered, and the carrier is removed using a phase tracking loop. The DLL (Delay-Locked Loop) retrieves the navigation data for code synchronization. This paper aims to model an L1 GPS signal receiver and assess its performance in both the time and frequency domains. The processing of this evaluation is regarding input dynamics such as Doppler and noise. This study emphasizes the importance of the Gold code with respect to cross-correlation and autocorrelation compared to the traditional PN coding. When it comes to wireless networks, Gold code is an interesting option since it can produce a more restricted and stable spectrum than PN code. The results demonstrate how a DLL with a narrow bandwidth may still decode data even if the system loses tracking, giving the system a higher level of reliability.

تقييم اداء ونمذجة مستلم نظام الموقع الشامل وتتبع الموجة

عبدالله خالد احمد، محمد المحمدي، ناصر الفلاحي
قسم الهندسة الكهربائية / كلية الهندسة / جامعة الأنبار / الانبار - العراق.

الخلاصة

يتمتع طيف انتشار التسلسل المباشر (DSSS) بحصانة كبيرة ضد الضوضاء بسبب كسب الانتشار العالي لرمز الضوضاء الزائفة (PN). تبث الاقمار الصناعية التابعة لمنظومة تحديد المواقع رسائل ضمن ترددات حزمة L1, هذه الاشارات تتضمن رمز الاستحواذ الخشن. لتتبع بيانات الملاحة، يتم تقييم سيناريوهين: عملية تتبع الطور وعملية تتبع الرمز. حلقة تتبع الطور تستخدم لإزالة الموجة الحاملة واستعادة البيانات المشفرة. حلقة التأخير المقفل (DLL) تستخدم لمزامنة الشفرة لاستعادة بيانات الملاحة. هدف هذا العمل يتضمن تصميم مستقبل إشارة L1 GPS لتقييم الأداء في مجالات الوقت والتردد. هذا التقييم تم تنفيذه بالأخذ بالحسبان تغيرات الادخال كالضوضاء والدوبلر. هذا العمل يوضح اهمية شفرة كولد من حيث الارتباط الذاتي والارتباط المتبادل، مقارنة بكود PN, مما يجعل شفرة كُولد مرشحًا واعدًا للشبكات اللاسلكية. توضح النتائج ميزة النطاق الترددي الضيق لـ(DLL) في فك تشفير البيانات حتى عندما يفقد النظام المسار، مما يعكس مؤشرا أكثر موثوقية للنظامً.

الكلمات الدالة: تتبع الناقل، تتبع الشفرة، شفرة كُولد، إشارة GPS، الضوضاء الزائفة.

1.INTRODUCTION

The Global Positioning System (GPS) provides an efficient and cost-effective approach to find the user's location, time, and velocity at anytime and anywhere [1]. GPS satellites transmit Course Acquisition (C/A) codes on L1P (Y), L2P (Y), and L1. GPS satellites were moved to Block IIR-M after 2005 (M-military), to which other codes were added, namely L1 (centered at 1575.42 MHz), L2 (centered at 1227.60 MHz), and L5 (centered at 1176.45 MHz), for greater accuracy [2, 3]. In addition, GPS added the C code on the L2 band to their codes for civilian use to improve positioning performance. Overall, 31 GPS satellites are on Medium Earth Orbit (MEO) at approximately 20,200 km height to provide navigation data 24/7 to users worldwide. The primary goal of a GPS receiver is to demodulate the navigation data and find the range between the receiver and the satellite. The transmitted navigation data, ephemerides, is a 50-bit-per-symbol code modulated with the Binary Phase Shift-Keying (BPSK) waveform and then coded with Gold Codes (GC). The transmitted ephemerides contain the satellite orbit parameters and clock, used in the ranging process and eventually positioning. The GPS signal is coded with Direct Sequence Spread Spectrum (DSSS) [4-6]. Ref. [7] presented Software Defined Radio (SDR) to tackle the low accuracy of the local oscillator used in the receiver. Tang et al. [8] presented that Fast Fourier Transform (FFT) decomposition can be applied to acquire signals faster. A more robust receiver was developed with a front-end architecture for the L1/L5 signal in Ref. [9]. Ref. [10] presented a faster acquisition process for the (C/A) GPS signal. The FFT algorithm was employed to depict the I/Q signals and the retrieved navigation data. Adaptive filtering is applied in Ref. [11] to minimize narrow-band jamming within the spread-spectrum signal. Reducing acquisition time is essential for GPS positioning. Ref. [12] developed an algorithm to decrease acquisition time and optimize computational complexity. Moreover, signal acquisition in a severe fading environment was studied in Ref. [1] using FFT, where the Adaptive Data Length (ADL) method was proposed to speed up the time for the acquisition. A low-complexity, weak signal tracking algorithm based on a sliding frequency lock loop for Global Navigation Satellite System (GNSS) signals in indoor environments was proposed by Ref. [13]. Savas et al. [14] compared different acquisition and tracking methods of GPS L1 C/A and GPS L5 signals in the presence of scintillations in the propagation environment. GPS-L5 signals in Ref. [15] calculated and verified a model for digital distortion and channel response. The tracking errors due to cycle slips at the receiver were studied in Ref. [16]. In another study, the Kalman filter was employed to enhance position estimates beyond the accuracy achieved through direct GPS measurements [17]. The Kalman filter was used as a post-processing technique to refine the precision of stand-alone SPS positioning in challenging scenarios [18, 19]. Wu et al. [20] examine four GPS L1/Galileo E1 models for common-clock receiver attitude determination. While the tightly coupled model had lower failure rates and higher ambiguity resolution (AR) success rates, the loosely combined model had outcomes in single-epoch mode that were identical to the double-differenced models. The single-differenced and tightly coupled models performed better in pitch accuracy and AR success rates in the multi-epoch mode. In another study, Bakuła et al. [21] used Huawei P30 Pro smartphones and a top-tier geodetic GNSS receiver (Javad Alpha) to investigate code differential GPS positioning. When comparing the P(L1) code to the P(L5) code, they discovered that the latter greatly reduced the accuracy of DGPS (Differential Global Positioning System) positions. There was a 60–80% reduction in the average horizontal and vertical coordinates errors. A smartphone with the P(L5) code had an accuracy of roughly 0.4 m (3D) while using 16 satellites and 0.3 m (3D) when using 26 satellites. Ref. [22] investigated the front-end design of GPS receiver systems, covering how GNSS and GPS are functioning alongside with architecture classification, image rejection methods, performance metrics,

and a new merit gauge for GPS receiver research, with its possible scope and difficulties. Nevertheless, Ref. [23] compared the noise level and performance of low-cost GNSS receivers with geodetic ones. It also suggested a dual low-cost rover system to lower noise and increase precision, thereby expanding the use of these devices in network monitoring applications. Another research investigated the characteristics of the GPS L2C signal for upcoming positioning algorithms. Modernized satellite quality metrics were compared using C/A and P2(Y) codes. The (24 reference) stations' worth of experimental data from expensive and high-end receivers were used for quality analyses. The results demonstrate that L2C-derived measures are superior to the encoded army signal but equal to the legacy public code [24]. Moreover, Yoon et al. [25] presented a geometry-based method to identify simultaneous cycle slips in several satellite channels using a single-frequency receiver. By detecting a half-wavelength cycle slip for each channel, the method solved the problem of robust position determination in low signal reception conditions, such as urban regions. The present study models and simulates a coherent L1-carrier GPS receiver in the z-domain using MATLAB. Its performance is evaluated under high input dynamics such as the Doppler effect and noise, as presented in Fig. 1. The rest of the paper is structured as follows: the GPS signal model is clarified in Section 2, and the digital GPS receiver is illustrated in Section 3. Section 4 presents the system modeling, and the results are discussed, followed by the range processing in Section 5. Finally, the conclusions are drawn in Section 6.

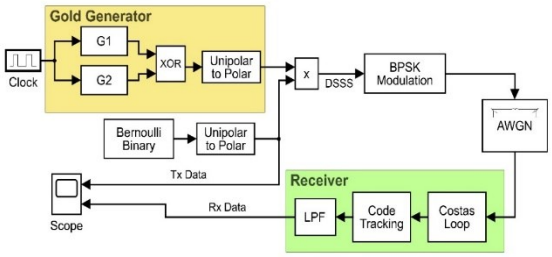

Fig. 1 The Transmission and Reception of GPS Signals.

2.GPS SIGNAL MODEL

DSSS signaling, which is used in GPS, is a signal that uses a larger bandwidth in modulation than that required by the underlying data modulation. Generally, a spread spectrum system is useful in managing interference, making interception by unauthorized listeners much more difficult, accommodating multi-path, and providing multiple access capabilities [26]. The DSSS signal is generated by directly mixing the data with a spreading code before the carrier modulation. A direct-sequence signal with BPSK or differential PSK (DPSK) modulation is represented by Eq. (1), and the spreading waveform is represented by Eq. (2) [27]:

$$s(t) = A\, d(t)\, c(t) \cos(2\pi\omega_c t + \theta) \quad (1)$$

$$c(t) = \sum_{i=-\infty}^{\infty} c_i\, \psi(t - iT_c) \quad (2)$$

where A is the amplitude of the signal, $d(t)$ is the binary data, $c(t)$ is the spreading waveform, ω_c is the carrier frequency, θ is the phase, T_c is the chip duration of the code, ψ is the correlation, and t is the time. The coherent BPSK DSSS receiver collects the received signal by multiplying it with a copy of the spreading code $c(t)$ [28]. The de-spreading process is successful only if the receiver code is synchronized with the received signal's spreading code. Here, the autocorrelation function and the autocorrelation of an infinite sequence are calculated using Eq. (3) and Eq. (4), respectively.

$$R_c(\tau) = \lim_{A\to\infty} \frac{1}{2A} \int_{-A}^{A} c(t)c(t-\tau)dt \quad (3)$$

$$R(\tau) = \begin{cases} 1 - |\tau|, & \text{for } |\tau| \le T_c \\ 0, & \text{otherwise} \end{cases} \quad (4)$$

where τ is the time shift of the correlation.

The chipping rate for the L1 C/A code is 1.023 Mbps. The GC family is used to form C/A codes. In GCs, two Pseudo Noise (PN) codes are summed together to provide lower cross-correlation than a single PN code. In this context, each GPS satellite has its unique C/A code, each with 1023 chip PN codes generated from a 10-bit shift register. G_1 and G_2 have initial seeds of "1's. Also, the tap positions of G_1 and G_2 are taken from the following generating polynomials [29]:

$$G_j = G_1(10) + G_2(s_{j1}) + G_2(s_{j2}) \quad (5)$$

where $G_1 = 1 + x^3 + x^5$ and $G_2 = 1 + x^2 + x^3 + x^6 + x^8 + x^9 + x^{10}$ G_j, in Eq. (5), are the sequence of the GC for the jth satellite, s_{j1} and s_{j2} are the tap values of the signal predefined for the j^{th} satellite and x represents the position of the flip-flop in the shift register. In the GPS signal, the frequency of the PN code C/A is 1.023 MHz, and the period is 1023 bits (1μs) per chip. The navigation message, which has a frequency of 50 Hz, is broadcast using the PN code [30]. The C/A signal is then BPSK-modulated and transmitted across the communication channel using a carrier with a frequency of 1575.42 MHz (L1 band). Although GCs have a far lower cross-correlation than PN sequence codes, they have the same autocorrelation. The auto and cross-correlations of a GC are plotted in Fig. 2(a) and Fig. 2(b), respectively. The autocorrelation of GC has a very high main peak with very low spikes, as shown in Fig. 2(a). However, GCs have very low cross-correlations between their individual codes, demonstrating low interference among GCs, as illustrated in Fig. 2(b).

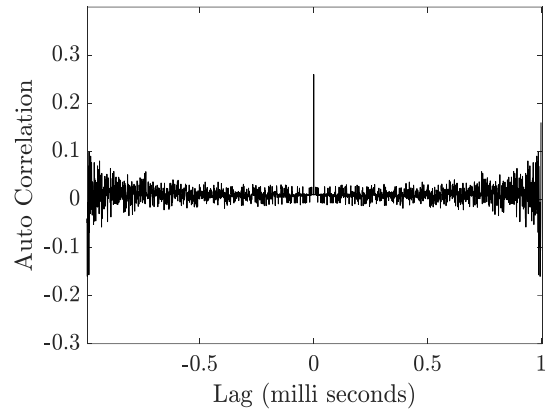

(a)

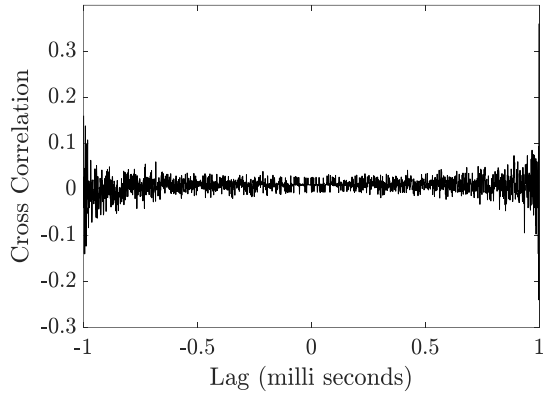

(b)

Fig. 2 Correlation of GC: (a) Autocorrelation and (b) Cross-Correlation.

3.DIGITAL GPS RECEIVER

3.1.GPS Signal Acquisition

Signal acquisition is the first task of a GPS receiver. The acquisition process is the ability of the receiver to identify the satellites and catch the C/A code. This task is challenging, especially as the user moves at high speed, which amplifies the Doppler effect. The relative motion of the satellite and the receiver causes the frequency to shift up or down the carrier frequency of the L1 band. The phase is the time difference of the C/A code in the received signal compared to the code generated locally. The receiver must align its local C/A code with the received (shifted) code to decode the received signal and extract the transmitted data [12].

3.2.GPS Signal Tracking

The main task of signal tracking is to refine the frequency change and code shift parameters and demodulate the received data. In this context, the navigation data is multiplied by a carrier replica of the BPSK to demodulate the signal. After that, the demodulated signal is multiplied with a synchronized GC to remove the code from the navigation data. The output of this system yields navigation data. Therefore, the tracking system should generate two synchronized signals, one for the BPSK carrier and the other for the GC DSSS, to perfectly receive the navigation data from the designated satellite [14, 31, 32].

3.2.1.Carrier Tracking

A modified Phase Lock Loop (PLL), called the Costas loop, is often used. It generates a replica of the BPSK carrier to demodulate the navigation data successfully. A block diagram for the Costas loop used in the simulation of this paper is presented in Fig. 4(a). The Costas loop adopts maximum likelihood estimation in the phase detector [33]. The loop has two branches: I and Q, where I represents the output data, and Q represents the error (called the lock indicator). The demodulated data will be presented on the loop's I-branch after the low pass filter (LPF) while the loop works in lock mode. The Costas loop is used over the default PLL loop because it can handle 180° phase shifts and keeps the signal tracking [34, 35].

3.2.2.Code Tracking

The primary task of the code tracking loop, depicted in Fig. 4(b), is to track the phase of the received signal. The code tracking loop uses a modified PLL system called the Delay Lock Loop (DLL) [36]. It generates three code replicas: Early (E), Prompt (P), and Late (L) codes. These two local code reference signals power the two independent correlators (Early and Late). They share the same frequency but differ in time delay [37]. Because E and L are fixed and cannot be adjusted at the beginning of the operation, the error signal must travel through a loop filter before approaching the VCO [36]. The VCO shifts its free-running frequency up or down to modify the clock frequency of the E, P, and L codes. This process is replicated until the error signal is zero or the subtraction of the codes E and L is zero. The purpose of this scenario is to indicate that the received code matches its replica produced by the receiver or that the received code is in sync with the P-code. Once the matching process has occurred, the P-code can provide the transmitted message modulated and encoded at the transmitter. Using the DLL, the receiver can predict the pseudo-range between the transmitter and receiver, a critical parameter in calculating the true range and ultimately determining the receiver's position [38]. The Costas loop and the DLL are second-order systems with loop filters. The transfer function of the loop filter is represented in Eq. (6) [39]:

$$F(z) = \frac{(K_0K_1(C_1+C_2)z^{-1} - K_0K_1C_1z^{-2})}{1+[K_0K_1(C_1+C_2)-2]z^{-1}+(1-K_0K_1C_1)z^{-1}} \quad (6)$$

$$C_1 = \frac{1}{K_0K_1}\frac{8\zeta\omega_n t_s}{4+4\zeta\omega_n t_s+(\omega_n t_s)^2}$$
$$C_2 = \frac{1}{K_0K_1}\frac{4(\omega_n t_s)^2}{4+4\zeta\omega_n t_s+(\omega_n t_s)^2} \quad (7)$$

where ζ is the system damping factor, ω_n is the natural frequency in rad/sec, K_0 and K_1 are the gains of the two loops, and t_s is the sampling time used in the system.

4.SYSTEM MODELING

The reception of GPS signals starts with carrier tracking through the Costas loop, which is a crucial step to operate. The receiver must maintain tracking to receive the GPS signal correctly. Once the carrier tracking is initialized, the GPS receiver must track the GC deployed in the received signal, achieved through the DLL, which is necessary to decode the data to extract the navigation information. These processes can be presented as a flowchart in Fig. 3. The models of the carrier- and code-tracking loops are detailed in Fig. 4. In the following part, we discuss the signal dynamics within these systems. In the Costas loop, the I-branch "in phase" is responsible for removing the carrier from the BPSK signal; this delivers the navigation data spread by the GC. The Q-branch "Quadrature phase" is considered the lock indicator, as it generates a signal related to the state of the loop, whether it is locked or not.

5.SIMULATION RESULTS

5.1.Carrier Tracking

The carrier tracking loop takes some time to achieve carrier acquisition, as shown in Fig. 5(a). The output in the I-branch is the navigation data spread by the GC, which settled down within Ts (the settling time, whose value depends on the type of signal and cycle slipping). As illustrated in Fig. 5(b), Ts is about 2 milliseconds. In this figure, a noise-like signal is shown by the lock indicator (Q-branch), and if there is an error in the Q-output, this signal continues, meaning that the loop has not yet acquired a lock. Lock acquisition is accomplished when this noise approaches zero. In this case, the loop's center frequency is shifted 10 kHz from the L1 signal.

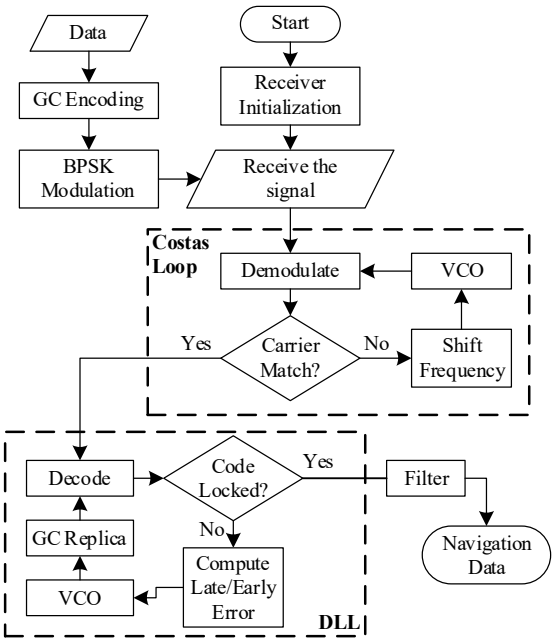

Fig. 3 Flowchart for the Reception of the GPS Signal.

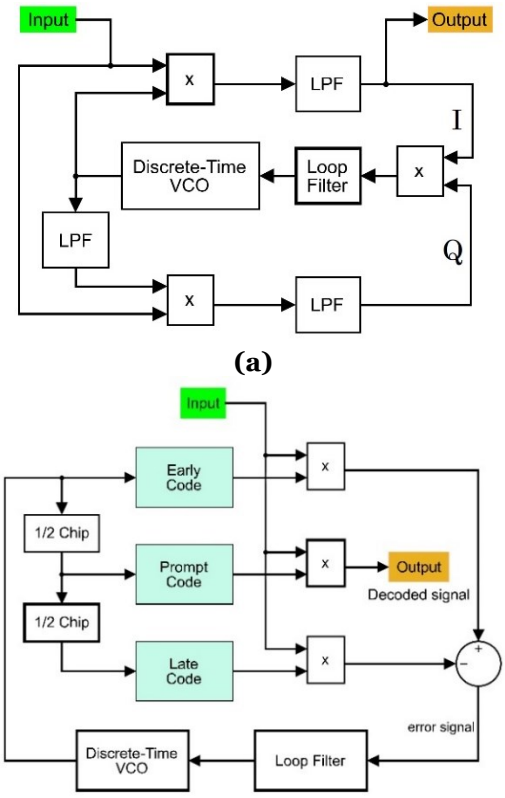

Fig. 4 Modeling of GPS L1 Signal Tracking: (a) Carrier Tracking Loop, and (b) Code Tracking Loop.

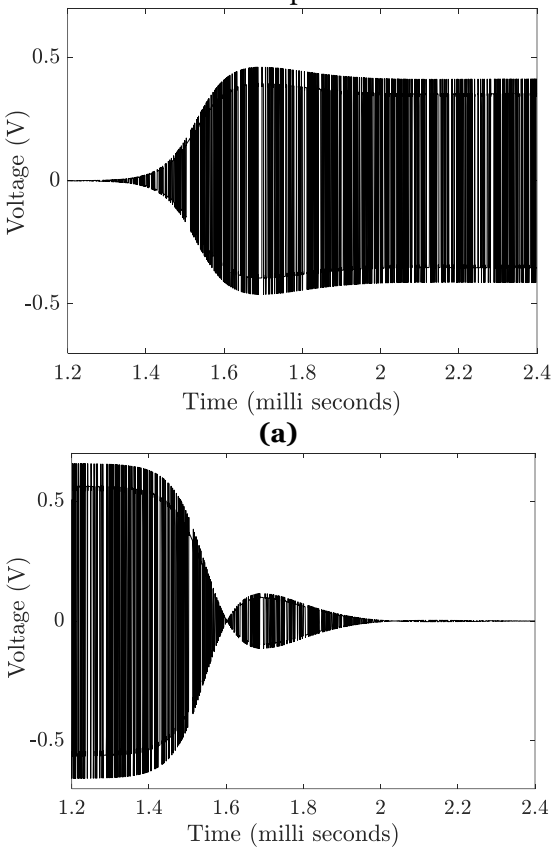

Fig. 5 Carrier Tracking Loop: (a) Signal I: in-Phase Signal, and (b) Signal Q: Quadrature Signal.

Due to the input dynamics, such as the Doppler effect, the input signal is shifted from the designated frequency. Therefore, the tracking loop must shift its center frequency to track the change. Cycle-slip takes place when the center frequency of the loop is “very distant” from the carrier frequency of the received signal. As a result, the lock indicator shows, for several cycles, a noise-like signal. Finally, when the two frequencies match, the output from the lock indicator becomes zero. The error signal generated by the phase detector is filtered by the loop filter, which is then applied as input to the Voltage Controlled Oscillator (VCO). The VCO detunes the loop frequency (shift up or down) by a rate determined by its sensitivity (Kvco). As a result, the generated local frequency follows the frequency deviations of the input signal. The VCO's sensitivity is set as a design requirement at 1000 Hz/Volt. Since the loop can modify its frequency to meet the change (after slipping a few cycles), the system can similarly adapt its operation to account for the Doppler shift in the received signal. When the center frequencies of the reception and carrier tracking loop are equal, the system operates in normal mode as an ordinary second-order system.

5.2.Code Tracking

The code tracking loop employs an Early-Late-gate DLL and attempts to synchronize its local GC with the incoming code, which has an unidentified delay caused by wave propagation from the satellite to the receiver. For these three branches, i.e., E-, L-, and P-codes, this loop generates the identical GC sequence used to generate the DSSS in the transmitter. The E branch arrives "before" (or earlier) than the incoming signal because it is intended to have no delay. The P arrives "before" or "after" the incoming signal due to its half-chip delay. Lastly, the L branch has a full chip delay that will undoubtedly arrive "after" the received code (late), as shown in Fig. 6(a), which shows the time domain of E, P, and L signals. The difference in reception between E and L codes will be filtered, and then it is employed as the controlling signal for the discrete VCO to adjust its frequency that clocks the shift registers. The E and L signals are employed as guards to the right and left of the desired code until the error signal (E-L) is minimized or settles to zero. In this case, the error signal will display as zero output, indicating that no further modification is necessary. Now, this P branch has caught the received code. This synchronization will enable the extraction of navigational data. Fig. 6(b) shows the frequency domain spectrum of E, P, and L signals. The correlations between the input and the three codes are shown in Fig. 7. This figure demonstrates that the P-code and the received code correlate best because they have the least time difference compared with the E and L codes. The E–L difference is mainly employed as a modulating control signal for the VCO. The P code will be used to retrieve the navigational data once the DLL loop has acquired the lock, as depicted in Fig. 8(a). Because of the high sampling rate used in the system, rapid fluctuations in values within each bit of the recovered navigation data are expected. Figure 8 (b) plots the frequency domain of the navigation data before and after the de-spreading process with the P-code.

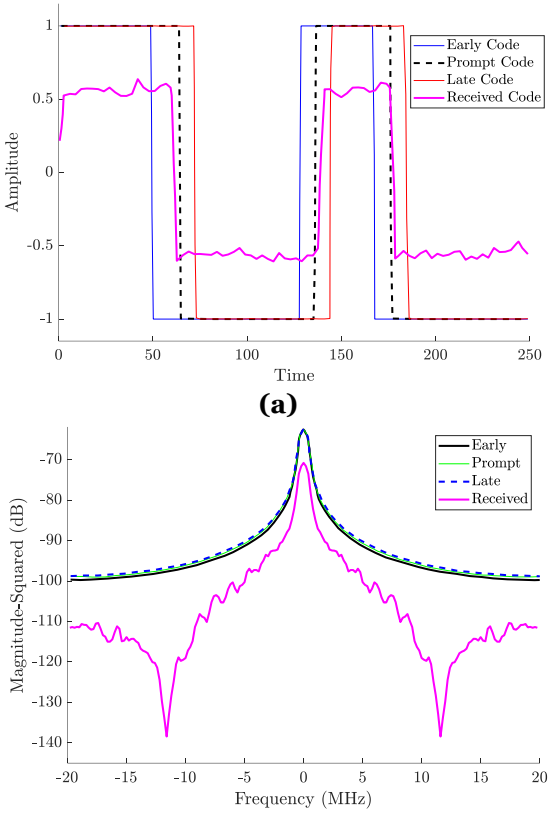

Fig. 6 The E, L, and P Codes of the Received Code: (a) Time Domain and (b) Frequency Domain.

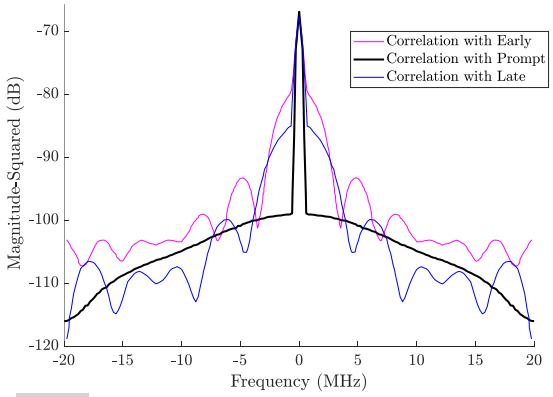

Fig. 7 Correlation of the Received Code with E, L, and P Codes.

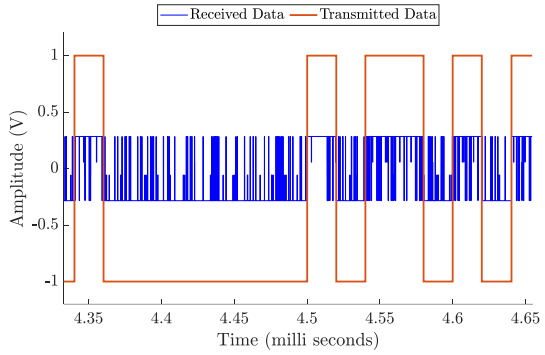

(a)

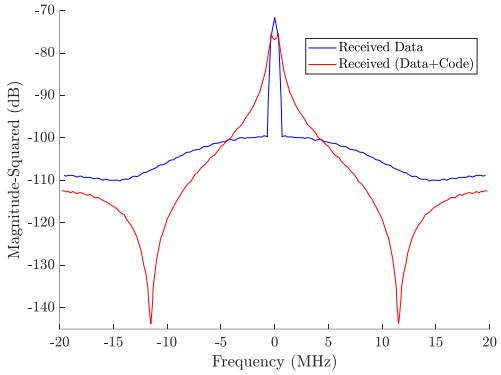

(b)

Fig. 8 The Transmitted and Recovered Navigation Data: (a) Time Domain and (b) Frequency Domain.

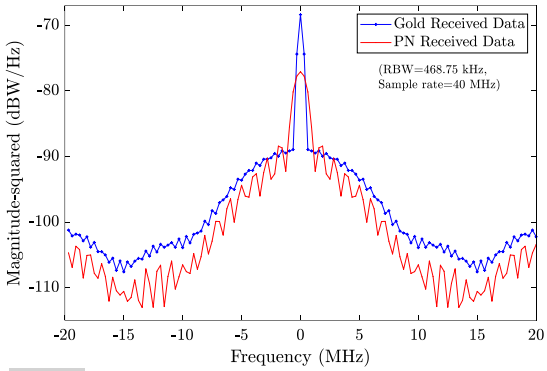

Fig. 9 Received Data Using GC vs. PN Code.

6.RANGE PROCESSING AND ESTIMATION

To enable GPS users to determine their precise location, they need to know the position of the satellites and the range of each satellite. Pseudo-ranging is employed, whereby a GPS user determines an estimated distance between themselves and the satellite by correlating a local code and a satellite code within the receiver. The signal's traveled distance can be calculated by multiplying the velocity of the satellite signal's transmission by the elapsed transmission time, considering any alterations to the satellite signal's velocity caused by tropospheric and ionospheric conditions. All shift registers' outputs are applied as inputs to an AND gate. The detected "all-one" state will be used to control the operation of the range estimator. This signal is named either "over-flow" or "strobe," according to which block is used for the determination. The "over-flow" is generated using the G1 coder inside the Prompt block within the code tracking loop.

On the other hand, to obtain the "strobe" signal, a PN code identical to that generated in the satellite is generated. The exact timing of this local code is gathered from the time information within the received data. The G1 branch for this code is used to generate the "strobe." Figure 10 illustrates a common method of range processing, which involves employing a delay estimation technique and a PN code tracking loop. The counter is 12-bit with a 10 MHz clock resolution. The overflow signal provides the reset signal for this counter. The strobe is used as a clock to activate a buffer linked to the counter's output. Consequently, when the buffer receives the strobe, it transfers the counter's data (final count), representing the time delay. The range is calculated by multiplying the received time delay by the speed of light, representing the distance between the user and the designated satellite.

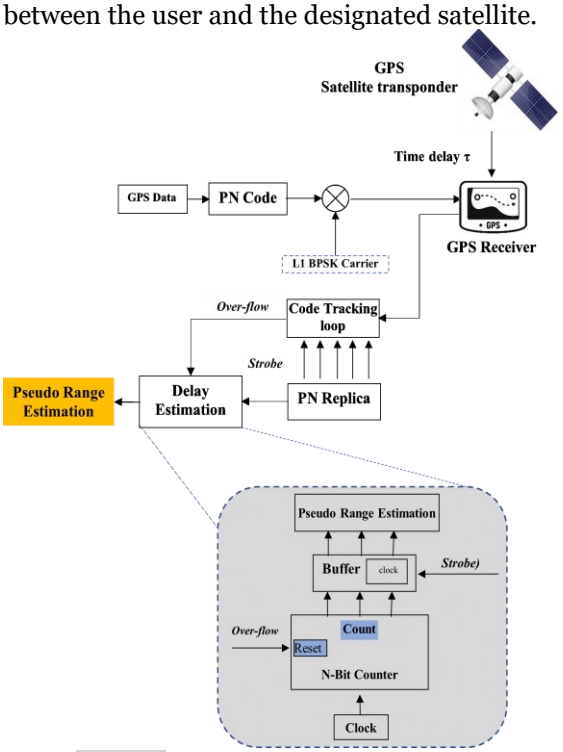

Fig. 10 The PN Range Estimation.

7.CONCLUSIONS

The primary findings of the current research can be succinctly stated as follows:

- Using GCs (modified PN) significantly improves the performance of the GPS receiver. As the results demonstrated, the cross-correlation of GCs is very low. Therefore, such codes enable several satellites to operate without interference.
- The present paper depicted that GPS receivers can automatically track the Doppler shift within the incoming signals. In noisy channels, the code tracking loop

can continue to decode the received code and deliver navigation messages even if the carrier tracking loop loses the reception lock and even during cycle slipping, which is a significant benefit of using this receiver in a noisy environment.

- GC can significantly improve signal reception and recovery performance. The received navigation data is also significantly improved, and the data signal is stable and bounded compared with PN codes, making GC a promising candidate for the next generation of wireless networks.

ACKNOWLEDGEMENTS

This work is fully supported by the authors.

NOMENCLATURE

A	Amplitude, Volts
$c(t)$	Spreading waveform, Volts
G_j	The sequence of the GC
K_0	Gain of loop 1
K_1	Gain of loop 2
$R_c(\tau)$	Autocorrelation function
t	Time, seconds
T_c	Chip duration of the code, seconds
t_s	Sampling time, seconds
Ts	Settling time, seconds
x	Position of the flip flop in the shift register
Greek Symbols	
θ	Phase, rad
ω_c	Carrier frequency, rad/s
ω_n	Natural frequency, rad/s
ζ	The damping factor
τ	The time shift of the correlation, seconds
ψ	Correlation
Subscripts	
c	Carrier
j	Satellite
n	Natural
s	Sampling

REFERENCES

[1] Hussain A, Ahmed A, Magsi H, Soomro JB, Bukhari SSH, Ro JS. **Adaptive Data Length Method for GPS Signal Acquisition in Weak to Strong Fading Conditions**. *Electronics* 2021; **10**(14):1653.

[2] Allen DW, Arredondo A, Barnes DR, Betz JW, Cerruti AP, Davidson B, Kovach KL, Utter A. **Effect of GPS III Weighted Voting on P(Y) Receiver Processing Performance**. *Navigation* 2020; **67**(4):675-689.

[3] de O. Moraes A, Vani BC, Costa E, Sousasanto J, Abdu MA, Rodrigues F, Gladek YC, de Oliveira CBA, Monico JFG. **Ionospheric Scintillation Fading Coefficients for the GPS L1, L2, and L5 Frequencies**. *Radio Science* 2018; **53**(9):1165-1174.

[4] Zhang Z, Lei J. **A Detecting Algorithm of DSSS Signal Based on Auto-Correlation Estimation**. *2017 IEEE 2nd Advanced Information Technology, Electronic and Automation Control Conference (IAEAC)*; 2017 March 25-26; Chongqing, China. pp. 137-141.

[5] Aljumaili M. **Modeling the Dielectric Mediums Impact on Coaxial Transmission Line Performance**. *Journal of Engineering and Applied Sciences* 2018; **13**(10):8419-8425.

[6] Zhang S, Liu F, Huang Y, Meng X. **Adaptive Detection of Direct-Sequence Spread-Spectrum Signals Based on Knowledge-Enhanced Compressive Measurements and Artificial Neural Networks**. *Sensors* 2021; **21**(7):2538.

[7] Lin S-S, Li Y-H. **A SDR-Based GPS Receiver with Low Accuracy of Local Oscillator**. *2021 International Symposium on Intelligent Signal Processing and Communication Systems (ISPACS)*; 2021 November 16-19; Hualien, Taiwan. pp. 1-2.

[8] Tang C, Wen T, Liang Z, Xu X, Mou W. **Fast Acquisition Method Using Modified PCA with a Sparse Factor for Burst DS Spread-Spectrum Transmission**. *ICT Express* 2023; **9**(4): 589-594.

[9] La Valle RL, García JG, Roncagliolo PA. **A Dual-Band RF Front-End Architecture for Accurate and Reliable GPS Receivers**. 2018 IEEE/MTT-S International Microwave Symposium - IMS*; 2018 June 10-15; Philadelphia, PA, USA. pp. 995-998.

[10] Ruitao L, Songlin L, Gang L. **Research and Implementation of GPS Pseudo-Code Fast Acquisition Based on Matched Filter and FFT**. *2018 IEEE CSAA Guidance, Navigation and Control Conference (CGNCC)*; 2018 August 10-12; Xiamen, China. pp. 1-5.

[11] Ali SH. **Suppression of the Narrow Band Jamming Signal in the Receiver of Spread Spectrum Communication System**. *Tikrit Journal of Engineering Sciences* 2013; **21**(2):19-23.

[12] Bahmani K, Nezhadshahbodaghi M, Mosavi MR. **Reduction of the Acquisition Time in GPS Receiver by Multi-Stage Frequency Bins**. *2020 10th International Symposium on Telecommunications (IST)*; 2020 December 16-18; Tehran, Iran. pp. 170-174.

[13] Liu X, Li J, Zhang Y. **The Algorithm of Weak Signal Tracking Based on Sliding Frequency Lock Loop**. *IET International Radar Conference (IET IRC 2020)*; 2020 November 4-6; Chongqing, China. pp. 807-811.

[14] Savas C, Falco G, Dovis F. **A Comparative Performance Analysis of GPS L1 C/A, L5 Acquisition and Tracking Stages under Polar and**

Equatorial Scintillations. *IEEE Transactions on Aerospace and Electronic Systems* 2021; **57**(1):227-244.

[15] Wang M, Lu X, Rao Y. **GNSS Signal Distortion Estimation: A Comparative Analysis of L5 Signal from GPS II and GPS III**. *Applied Sciences* 2022; **12**(8):3791.

[16] Beeck SS, Mitchell CN, Jensen AB, Stenseng L, Pinto Jayawardena T, Olesen DH. **Experimental Determination of the Ionospheric Effects and Cycle Slip Phenomena for Galileo and GPS in the Arctic**. *Remote Sensing* 2023; **15**(24):5685.

[17] Deep A, Mittal M, Mittal V. **Application of Kalman Filter in GPS Position Estimation**. *2018 IEEE 8th Power India International Conference (PIICON)*; 2018 December 10-12; Kurukshetra, India. pp. 1-5.

[18] Kumalasari IN, Zainudin A, Pratiarso A. **An Implementation of Accuracy Improvement for Low-Cost GPS Tracking Using Kalman Filter with Raspberry Pi**. *2020 International Electronics Symposium (IES)*; 2020 September 29-30; Surabaya, Indonesia. pp. 123-130.

[19] Agarwal N, Keefe KO. **Use of GNSS Doppler for Prediction in Kalman Filtering for Smartphone Positioning**. *IEEE Journal of Indoor and Seamless Positioning and Navigation* 2023; **1**:151-160.

[20] Wu M, Li J, Luo S, Liu W. **Attitude Determination with GPS L1/Galileo E1 Observations from Common-Clock Receiver: A Comparison of Four Different Models**. *Remote Sensing* 2022; **14**(21):5438.

[21] Bakuła M, Uradziński M, Krasuski K. **Performance of DGPS Smartphone Positioning with the Use of P(L1) Vs. P(L5) Pseudorange Measurements**. *Remote Sensing* 2022; **14**(4):929.

[22] Kumari A, Bhatt D. **Advanced System Analysis and Survey on the GPS Receiver Front End**. *IEEE Access* 2022; **10**:24611-24626.

[23] Xue C, Psimoulis P, Zhang Q, Meng X. **Analysis of the Performance of Closely Spaced Low-Cost Multi-GNSS Receivers**. *Applied Geomatics* 2021; **13**(3):415-435.

[24] Yun S, Lee H. **Experimental Analysis of GPS L2C Signal Quality under Various Observational Conditions**. *International Journal of Geoinformatics* 2022; **18**(3):21-37.

[25] Yoon Y-M, Lee B-S, Heo M-B. **Multiple Cycle Slip Detection Algorithm for a Single Frequency Receiver**. *Sensors* 2022; **22**(7):2525.

[26] Robson S, Haddad M. **A Chirp Spread Spectrum Modulation Scheme for Robust Power Line Communication**. *IEEE Transactions on Power Delivery* 2022; **37**(6):5299-5309.

[27] Choi H, Moon H. **Blind Estimation of Spreading Sequence and Data Bits in Direct-Sequence Spread Spectrum Communication Systems**. *IEEE Access* 2020; **8**:148066-148074.

[28] Mohammed Salih A. **Secured Watermarking Image Using Spread Spectrum**. *Tikrit Journal of Engineering Sciences* 2016; **23**(3):71-78.

[29] Kim M, Park J, Jo G, Yoo H. **Area-Efficient Universal Code Generator for Multi-GNSS Receivers**. *Electronics* 2021; **10**(20):2485.

[30] Kim ST, Ahn JM. **Analysis of Correlation Characteristics of 10230 Period PRN Code Using Concatenated Gold Code**. *2019 International Conference on Electronics, Information, and Communication (ICEIC)*; 2019 January 22-25; Auckland, New Zealand. pp. 1-2.

[31] Pei Y, Chen H, Pei B. **Implementation of GPS Software Receiver Based on GNU Radio**. *2018 Cross Strait Quad-Regional Radio Science and Wireless Technology Conference (CSQRWC)*; 2018 July 21-24; Xuzhou, China. pp. 1-3.

[32] Zeng Y, Yu Y, Liu L. **Realization of Baseband Signal Processing for Beidou/GPS Multi-Mode Receiver by FPGA**. *2017 IEEE 9th International Conference on Communication Software and Networks (ICCSN)*; 2017 May 6-8; Guangzhou, China. pp. 860-864.

[33] Vilnrotter V, Cheung KM. **Near-Optimum Real-Time Range Estimation Algorithms for Proximity Links**. *2021 IEEE Aerospace Conference (50100)*; 2021 March 6-13; Big Sky, MT, USA. pp. 1-11.

[34] Yang R, Huang J, Zhan X, Luo S. **Decentralized FLL-Assisted PLL Design for Robust GNSS Carrier Tracking**. *IEEE Communications Letters* 2021; **25**(10):3379-3383.

[35] Wali SA, Muhammed AA. **Power Sharing and Frequency Control in Inverter-Based Microgrids**. *Tikrit Journal of Engineering Sciences* 2022; **29**(3):70-81.

[36] Beldjilali B, Benadda B. **Real Time Software Based L1 C/A GPS Receiver**. *2017 Seminar on Detection Systems Architectures and Technologies (DAT)*; 2017 March 20-22; Algiers, Algeria. pp. 1-8.

[37] Li J, Zhao L, Hou Y, Hu Y. **A New Tracking Technique with the Memory Discriminator for High Sensitivity GNSS Receivers**. *2018 IEEE 4th International Conference on Computer and Communications (ICCC)*; 2018 December 7-10; Chengdu, China. pp. 959-962.

[38] Zhou F, Wang X. **Some Key Issues on Pseudorange-Based Point Positioning with GPS, BDS-3, and Galileo Observations**. *Remote Sensing* 2023; **15**(3):797.

[39] The MathWorks Inc. **Phase-Locked Loops - Loop Filter**. 2024. Available from: https://www.mathworks.com/help/msblks/ref/loopfilter.html